Functional Assessment of the *Medicago truncatula* NIP/LATD Protein Demonstrates That It Is a High-Affinity Nitrate Transporter[1][W][OA]

Rammyani Bagchi[2], Mohammad Salehin[2], O. Sarah Adeyemo, Carolina Salazar, Vladimir Shulaev, D. Janine Sherrier, and Rebecca Dickstein*

Department of Biological Sciences, University of North Texas, Denton, Texas 76203 (R.B., M.S., O.S.A., C.S., V.S., R.D.); and Department of Plant and Soil Sciences, Delaware Biotechnology Institute, University of Delaware, Newark, Delaware 19711 (D.J.S.)

The *Medicago truncatula NIP/LATD* (for Numerous Infections and Polyphenolics/Lateral root-organ Defective) gene encodes a protein found in a clade of nitrate transporters within the large NRT1(PTR) family that also encodes transporters of dipeptides and tripeptides, dicarboxylates, auxin, and abscisic acid. Of the NRT1(PTR) members known to transport nitrate, most are low-affinity transporters. Here, we show that *M. truncatula nip/latd* mutants are more defective in their lateral root responses to nitrate provided at low (250 μM) concentrations than at higher (5 mM) concentrations; however, nitrate uptake experiments showed no discernible differences in uptake in the mutants. Heterologous expression experiments showed that *MtNIP/LATD* encodes a nitrate transporter: expression in *Xenopus laevis* oocytes conferred upon the oocytes the ability to take up nitrate from the medium with high affinity, and expression of *MtNIP/LATD* in an Arabidopsis *chl1(nrt1.1)* mutant rescued the chlorate susceptibility phenotype. *X. laevis* oocytes expressing mutant *Mtnip-1* and *Mtlatd* were unable to take up nitrate from the medium, but oocytes expressing the less severe *Mtnip-3* allele were proficient in nitrate transport. *M. truncatula nip/latd* mutants have pleiotropic defects in nodulation and root architecture. Expression of the Arabidopsis *NRT1.1* gene in mutant *Mtnip-1* roots partially rescued *Mtnip-1* for root architecture defects but not for nodulation defects. This suggests that the spectrum of activities inherent in AtNRT1.1 is different from that possessed by MtNIP/LATD, but it could also reflect stability differences of each protein in *M. truncatula*. Collectively, the data show that MtNIP/LATD is a high-affinity nitrate transporter and suggest that it could have another function.

All plants require nitrogen (N) as an essential nutrient and are able to acquire N from nitrate (NO_3^-) and ammonium (NH_4^+) in the soil. Nitrate acquisition begins with its transport into root cells, accomplished by NO_3^- transporters. Soil NO_3^- concentrations can vary by 5 orders of magnitude (Crawford, 1995), and to cope with the variability, plants have evolved both high-affinity (HATS) and low-affinity (LATS) transport systems. These are encoded by two gene families: the phylogenetically distinct NRT1(PTR) and NRT2 families. Members of these families also participate in the movement of NO_3^- throughout the plant and within plant cells (Miller et al., 2007; Segonzac et al., 2007; Tsay et al., 2007; Almagro et al., 2008; Lin et al., 2008; Fan et al., 2009; Li et al., 2010; Barbier-Brygoo et al., 2011; Wang and Tsay, 2011; Xu et al., 2012). Proteins in the Chloride Channel (CLC) transporter family also transport NO_3^-; these transporters are associated with cytosol-to-organelle NO_3^- movement (Zifarelli and Pusch, 2010).

NRT1(PTR) is a large family of transporters, comprising 53 members in Arabidopsis (*Arabidopsis thaliana*), 84 members in rice (*Oryza sativa*), with NRT1 (PTR) members known in several other species (Tsay et al., 2007; Zhao et al., 2010). In addition to transporting NO_3^- coupled to H^+ movement, members of the NRT1(PTR) family have been found to transport dipeptides or tripeptides, amino acids (Waterworth and Bray, 2006), dicarboxylic acids (Jeong et al., 2004), auxin (Krouk et al., 2010b), and/or abscisic acid (Kanno et al., 2012). Only a small number of NRT1 (PTR) proteins have been functionally studied compared with the large number that exist in higher plants; thus, the number of biochemical functions ascribed to this family may expand.

Of the NRT1(PTR) members known to transport NO_3^-, most are LATS transporters. An important exception is Arabidopsis NRT1.1(CHL1), a dual-affinity transporter that is the most extensively studied NRT1 (PTR) protein. *AtNRT1.1(CHL1)* was identified initially on the basis of its ability to confer chlorate toxicity

[1] This work was supported by the National Science Foundation (grant nos. IOS–0923756 to R.D. and IOS–0923668 to D.J.S.).

[2] These authors contributed equally to the article.

* Corresponding author; e-mail beccad@unt.edu.

The author responsible for distribution of materials integral to the findings presented in this article in accordance with the policy described in the Instructions for Authors (www.plantphysiol.org) is: Rebecca Dickstein (beccad@unt.edu).

[W] The online version of this article contains Web-only data.

[OA] Open Access articles can be viewed online without a subscription.

www.plantphysiol.org/cgi/doi/10.1104/pp.112.196444

resistance and was the first of this family to be cloned (Doddema et al., 1978; Tsay et al., 1993). AtNRT1.1 (CHL1) is an essential component of NO_3^- transport and NO_3^- signaling pathways, with important roles regulating the expression of other NO_3^- transporters and root architecture (Remans et al., 2006; Walch-Liu et al., 2006; Walch-Liu and Forde, 2008). Its expression is inducible by NO_3^- (Huang et al., 1996). Reversible phosphorylation is essential to its ability to switch between LATS and HATS activity (Liu and Tsay, 2003). In addition, AtNRT1.1(CHL1) acts as a NO_3^- sensor (Muños et al., 2004; Ho et al., 2009; Wang et al., 2009) and has been shown to transport auxin in a NO_3^- concentration-dependent manner (Krouk et al., 2010b). It has been suggested that AtNRT1.1's ability to transport auxin may be part of its NO_3^--sensing mechanism (Krouk et al., 2010a, 2010b; Gojon et al., 2011).

Most legumes and actinorhizal plants have the additional ability to form symbiotic N-fixing root nodules with soil bacteria, enabling them to thrive in NO_3^-- and NH_4^+-depleted environments. Legume nodulation commences with signal exchange between the plant and rhizobia, followed by root cortical cell divisions, invasion of the root by rhizobia inside plant-derived infection threads, and subsequent endocytosis of rhizobia into newly divided plant host cells, forming symbiosomes. Within symbiosomes, the rhizobia differentiate into bacteroids that are capable of N fixation (Oldroyd and Downie, 2008; Kouchi et al., 2010). Before N fixation begins, nodules are a sink for the plant's N; N is required to support nodule organogenesis and rhizobial proliferation and differentiation in nodules (Udvardi and Day, 1997). After N fixation begins, nodules are a source of bioavailable N and are a large carbon sink because of the energetic needs of the rhizobia that fix N (White et al., 2007).

NRT1(PTR) transporters have received less attention in legumes and actinorhizal plants than in other plants, but they are beginning to be investigated. Transcription patterns for several soybean (*Glycine max*) *NRT1*(*PTR*) transporter genes have been studied; they were predicted to encode transporters of NO_3^-, but were not characterized functionally (Yokoyama et al., 2001). Benedito et al. (2010) recognized 111 nonredundant *Medicago truncatula* sequences corresponding to genes in the 2.A.17 transporter class, containing NRT1(PTR) genes (Benedito et al., 2010). In *Lotus japonicus*, 37 members of the *NRT1*(*PTR*) family were identified by an in silico search (Criscuolo et al., 2012). The recent availability of three sequenced legume genomes will add to our knowledge of this important gene family (Sato et al., 2008; Schmutz et al., 2010; Young et al., 2011). In faba bean (*Vicia faba*), two NRT1(PTR) transporters have been studied; one was demonstrated to transport dipeptides in yeast, while the second was found to be phylogenetically close to a soybean NRT1(PTR) (Miranda et al., 2003). In alder (*Alnus glutinosa*) nodules, the NRT1(PTR) transporter AgDCAT localizes to the symbiotic interface and transports dicarboxylic acid from the cytosol toward its symbiotic partner, *Frankia* spp. (Jeong et al., 2004). The *M. truncatula* MtNRT1.3 transporter was shown to be a dual-affinity NO_3^- transporter; *MtNRT1.3* is up-regulated by the absence of NO_3^- (Morère-Le Paven et al., 2011).

The *M. truncatula NIP/LATD* (for Numerous Infections and Polyphenolics/Lateral root-organ Defective) gene encodes a predicted NRT1(PTR) transporter (Harris and Dickstein, 2010; Yendrek et al., 2010), and the three known *nip* and *latd* mutants have pleiotropic defects in nodulation and root architecture. *Mtnip-1*, containing a missense (A497V) mutation in one of the NIP/LATD protein's transmembrane domains, is well characterized with respect to nodulation phenotypes (Veereshlingam et al., 2004). *Mtnip-1* develops nodules that initiate rhizobial invasion but fail to release rhizobia from infection threads. Its nodules lack meristems and accumulate polyphenolics, a sign of host defense. *Mtnip-1* plants also have defective root architecture (Veereshlingam et al., 2004). The *Mtlatd* mutant has the most severe phenotype, caused by a stop codon (W341STOP) in the middle of the NIP/LATD putative protein (Yendrek et al., 2010). *Mtlatd* has serious defects in root architecture, with a nonpersistent primary root meristem, lateral roots (LRs) that fail to make the transition from LR primordia to LRs containing a meristem, and defects in root hairs. *Mtlatd* also has defective nodules (Bright et al., 2005). The missense *Mtnip-3* mutant (E171K) is the least affected, forming invaded nodules with meristems and polyphenol accumulation. *Mtnip-3* has nearly normal root architecture (Teillet et al., 2008; Yendrek et al., 2010).

Here, the function of the MtNIP/LATD protein is investigated. We find that MtNIP/LATD is a high-affinity NO_3^- transporter and provide evidence suggesting that it may have an additional biochemical function.

RESULTS

Mtnip Mutants' Nitrate Phenotypes

Because of MtNIP/LATD's similarity to low-affinity NO_3^- transporters in the NRT1(PTR) family (Yendrek et al., 2010), one hypothesis is that it may be a low-affinity NO_3^- transporter. Bioavailable N is known to suppress nodulation and to inhibit N fixation in mature N-fixing nodules (Streeter, 1988; Fei and Vessey, 2009). It is also possible that *Mtnip/latd* mutants would develop functional root nodules in conditions of NO_3^- sufficiency. To test whether *Mtnip-1* was altered in the suppression of nodulation by bioavailable N, *Mtnip-1* mutant plants were cultivated in 1 and 10 mM KNO_3 and also in 5 mM NH_4NO_3 in the presence of *Sinorhizobium meliloti*. As shown in Table I, *Mtnip-1* formed low numbers of nodules under these conditions compared with no-N conditions, similar to the wild type (A17), suggesting normal suppression by bioavailable N sources. The few nodules that formed in *Mtnip-1* in

Table I. *Nodulation in the absence and presence of N sources*

In each experiment, wild-type A17 and *Mtnip-1* plants were grown in the same aeroponic chamber in the given N regime, as described in "Materials and Methods." For each experiment, seven to 11 plants of each genotype were evaluated. Nodules were counted at 15 dpi. Data are presented as the mean number of nodules per plant ± SE.

Experiment	N Conditions	A17 Nodule No.	*Mtnip-1* Nodule No.
1	No NO_3	31. 9 ± 3.2	20.8 ± 1.6
2	No NO_3	19.9 ± 4.1	13.25 ± 0.8
3	1 mM KNO_3	7.8 ± 0.7	2.2 ± 0.4
4	1 mM KNO_3	5.3 ± 0.6	1.1 ± 0.3
5	5 mM NH_4NO_3	1.7 ± 0.6	0. 7 ± 0.2
6	5 mM NH_4NO_3	5.7 ± 0.6	2.8 ± 0.5
7	10 mM KNO_3	3.4 ± 0.8	0.6 ± 0.3
8	10 mM KNO_3	4.0 ± 1.0	0.7 ± 0.4

1 mM KNO_3, 10 mM KNO_3, or 5 mM NO_3NH_4 had an *Mtnip-1* nodule phenotype.

To examine whether the mutants had defects in NO_3^- uptake, we grew *Mtnip-1* and *Mtnip-3* mutants, with wild-type A17 as a control, in two different concentrations of KNO_3: 250 μM and 5 mM. Uptake was measured by monitoring the depletion of NO_3^- from the medium. As can be seen in Figure 1, no differences in NO_3^- uptake were observed in the mutants, suggesting that NO_3^- LATS and HATS are functioning in these plants. However, because measurement of the depletion of NO_3^- from the medium is less sensitive than measuring NO_3^- influx, subtle changes in NO_3^- uptake may not have been detected in this experimental system.

In Arabidopsis, growth of plants in different NO_3^- concentrations is known to affect root architecture (Zhang and Forde, 2000; Linkohr et al., 2002). To determine if *M. truncatula nip* mutants' LR phenotype was affected by NO_3^-, we grew *Mtnip-1*, *Mtnip-3*, and A17 in the presence of 0 μM, 250 μM, and 5 mM KNO_3 and examined root growth parameters after 2 weeks. Wild-type A17 produced longer LRs in both NO_3^- concentrations tested than it did at 0 NO_3^- and slightly shorter LRs in 5 mM as compared with 250 μM KNO_3 (Fig. 2). LR lengths of both *Mtnip-1* and *Mtnip-3* were significantly shorter than those of the wild type in all conditions tested, with one exception; in 5 mM KNO_3, the average LR lengths of *Mtnip-3* were similar to those of A17. Both *Mtnip-1* and *Mtnip-3* mutants had longer LRs when grown in 5 mM KNO_3 (Fig. 2C) than they did in 250 μM KNO_3 (Fig. 2B) and when grown in the absence of NO_3^- (Fig. 2A). These data are consistent with an MtNIP/LATD function in high-affinity, low-concentration NO_3^- uptake or response.

MtNIP/LATD Protein Transports Nitrate, But Not His, in *Xenopus laevis* Oocytes

To test whether the MtNIP/LATD protein transports NO_3^-, we expressed *MtNIP/LATD* in *X. laevis* oocytes and assayed them for the acquisition of NO_3^- transport activity. Transport activity was initially assessed at two different NO_3^- concentrations to categorize transporter affinity and at pH 5.5 and 7.4 to test pH dependence. As shown in Figure 3, A and B, oocytes expressing *MtNIP/LATD* were capable of significant NO_3^- uptake above the water-injected control oocytes at both low (250 μM) and high (5 mM) NO_3^- concentrations at pH 5.5. However, at pH 7.4, there was no significant NO_3^- uptake (Fig. 3, C and D), indicating that transport is H^+ coupled. We compared MtNIP/LATD NO_3^- transport with that of the dual-affinity AtNRT1.1 transporter and found that MtNIP/LATD had slightly lower nitrate transport than AtNRT1.1 at 250 μM NO_3^-. At 5 mM NO_3^-, MtNIP/LATD transported approximately 20% as much nitrate as did AtNRT1.1 (Supplemental Fig. S1), suggesting that MtNIP/LATD is not dual affinity. To determine MtNIP/LATD's K_m, we measured NO_3^- uptake in *MtNIP/LATD*-injected oocytes compared with water-injected control oocytes over NO_3^- concentrations ranging from 50 μM to 10 mM. MtNIP/LATD displays saturable kinetics for NO_3^- uptake, with a K_m of 160 μM (Fig. 3, E and F). The data show only one saturation point (Fig. 3E) and thus indicate that MtNIP/LATD has single, high-affinity NO_3^- transport.

Because the NRT1(PTR) family BnNRT1.2 NO_3^- transporter also transports His (Zhou et al., 1998), a rat

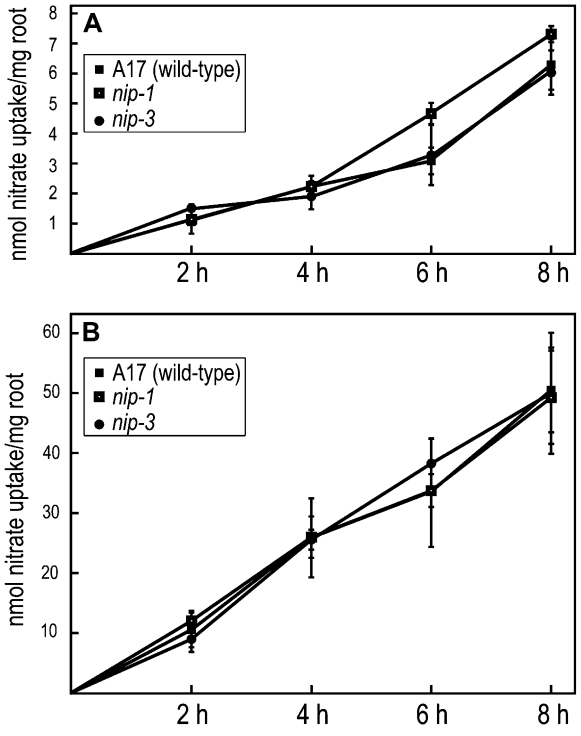

Figure 1. Nitrate uptake in *M. truncatula*. Wild-type A17, *Mtnip-1*, and *Mtnip-3* plants were placed in solutions containing 250 μM (A) or 5 mM (B) nitrate. Nitrate uptake was monitored by its depletion from the medium at 2-h intervals. Data are plotted for one biological replicate ± SE.

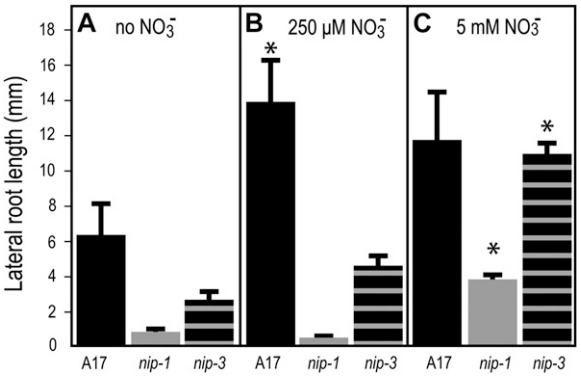

Figure 2. LR lengths of *M. truncatula* plants grown in different conditions. Wild-type A17 (black bars), *Mtnip-1* (gray bars), and *Mtnip-3* (horizontally striped bars) were grown in liquid buffered nodulation medium with no added NO_3^- (A), with 250 μM KNO_3 (B), or with 5 mM KNO_3 (C), with the medium changed every other day. LR lengths were measured after 2 weeks. Data are shown for one biological replicate ± SE ($n = 5$). Replicates gave similar results. Asterisks mark LR lengths from plants grown at 250 μM KNO_3 and 5 mM KNO_3 that are significantly different from the same genotype grown at 0 mM KNO_3, using Student's *t* test at $P < 0.05$.

NRT1(PTR) family member transports both peptides and His (Yamashita et al., 1997), and Arabidopsis AtPTR1 and AtPTR2 peptide transporters also transport His (Tsay et al., 2007), we assessed His uptake in *MtNIP/LATD*-injected oocytes compared with water-injected control oocytes. At pH 5.5 and 1 mM His, we observed no His transport (Supplemental Table S1).

Proteins Encoded by Two *MtNIP/LATD* Mutant Alleles But Not a Third Allele Are Defective in Nitrate Transport in the Oocyte System

The finding that MtNIP/LATD transports NO_3^- opens the possibility that the defects observed in the *Mtnip/latd* mutants result from defective NO_3^- transport. To determine if the proteins encoded by the available defective *MtNIP/LATD* genes are capable of NO_3^- transport, we tested them in the *X. laevis* oocyte system. The results demonstrate that the missense Mtnip-1 and truncated Mtlatd proteins are defective in NO_3^- transport at 5 mM NO_3^-, while the Mtnip-3 protein is capable of transport at this higher concentration (Fig. 4). Oocytes expressing Mtnip-3 protein as well as Mtnip-1 protein were assessed for high-affinity transport at 250 μM NO_3^-; since the Mtlatd protein, encoded by a gene with a nonsense codon in the middle of *MtNIP/LATD*, failed to transport NO_3^- at 5 mM NO_3^-, it was not tested for transport at 250 μM NO_3^-. Mtnip-3 was capable of transport at 250 μM, while Mtnip-1 was not. Because the *Mtnip-3* mutant has defective root architecture, aberrant nodulation, and fixes far less N than the wild type (Teillet et al., 2008), it may be defective in another function besides NO_3^- transport.

MtNIP/LATD Expression in the Arabidopsis *chl1-5* Mutant Restores Chlorate Sensitivity

Although MtNIP/LATD transports NO_3^- in oocytes, it could be argued that it may not function as a

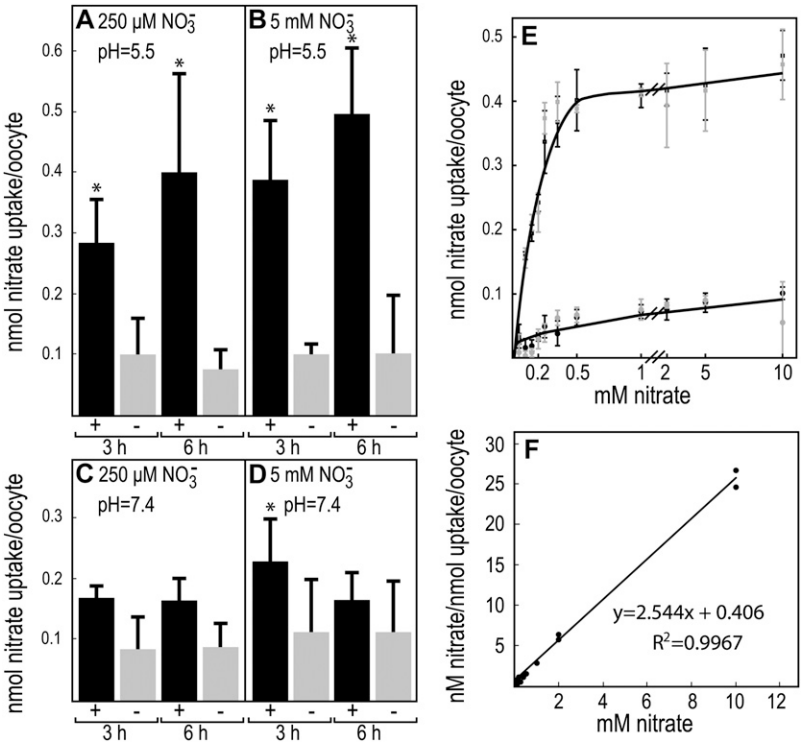

Figure 3. Nitrate uptake in *X. laevis* oocytes expressing *MtNIP/LATD*. Oocytes were microinjected with *MtNIP/LATD* mRNA (black bars, +) or water as a negative control (gray bars, −), incubated for 3 d, and then placed for the indicated times in medium containing 250 μM or 5 mM NO_3^- at pH 5.5 or 7.4. The oocytes were rinsed, lysed, and assayed for NO_3^- content. A and C, Treatment with 250 μM NO_3^-. B and D, Treatment with 5 mM NO_3^-. A and B, pH = 5.5. C and D, pH = 7.4. Data are shown for one biological replicate ± SD ($n = 3$–5 batches of 4–6 oocytes per batch). Asterisks mark NO_3^- uptake significantly different from the negative control, using Student's *t* test at $P < 0.05$. Similar results were obtained in more than five repetitions of the experiment. E, Michaelis-Menten plot of oocyte NO_3^- uptake. *MtNIP/LATD*-injected oocytes (squares) or water-injected oocytes (circles) as control were incubated for 3 h in 50 μM to 10 mM NO_3^- in batches of five and assayed for NO_3^- uptake. Results for two biological replicates are indicated by the black and gray symbols, with error bars showing SD. All NO_3^- uptake was significantly different from the negative control, using Student's *t* test at $P < 0.05$, except for that at 50 μM. F, Hanes-Woolf plot of averaged NO_3^- uptake data, in *MtNIP/LATD*-injected oocytes minus water-injected oocytes, presented in E. These data were used to calculate the K_m of 160 μM.

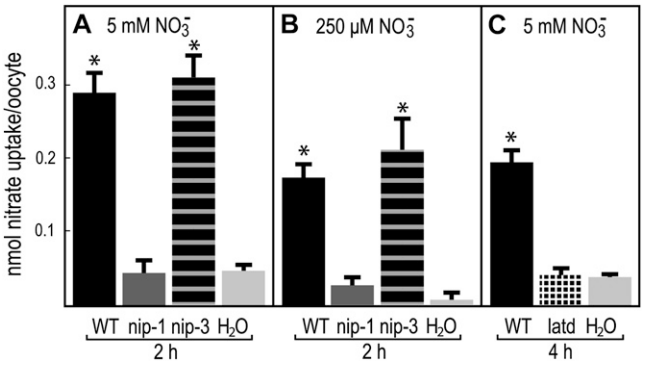

Figure 4. Nitrate uptake in *X. laevis* oocytes expressing *MtNIP/LATD* or mutant *Mtnip/latd* mRNAs. Oocytes were microinjected with *MtNIP/LATD* mRNA, mutant mRNA, or water as a negative control, incubated for 3 d, and then placed for the indicated times in medium containing 5 mM or 250 μM nitrate, at pH 5.5, and assayed for nitrate uptake. A, Treatment with 5 mM nitrate. B, Treatment with 250 μM nitrate. C, Treatment with 5 mM nitrate. Oocytes expressing wild-type (WT) *MtNIP/LATD* (black bars), *Mtnip-1* (dark gray bars), *Mtnip-3* (horizontally striped bars), *Mtlatd* (hatched bars), or water as a negative control (gray bars) are shown. Data are shown for one biological replicate ± SD (n = 3–5 batches of 4–6 oocytes per batch). Asterisks mark nitrate uptake that is significantly different from the negative control, using Student's t test at $P < 0.05$. Similar results were obtained in more than three repetitions of the experiment.

NO_3^- transporter in planta. The NO_3^- transporter activity of MtNIP/LATD was further tested by studying its ability to complement the well-characterized Arabidopsis *chl1-5* mutant, containing a large deletion in the *AtNRT1.1* gene (Muños et al., 2004). This mutant was originally isolated on the basis of its resistance to the herbicide chlorate, which is taken up through the AtNRT1.1(AtCHL1) NO_3^- transporter and reduced by NO_3^- reductase to toxic chlorite (Doddema et al., 1978; Tsay et al., 1993). A construct containing *MtNIP/LATD* cDNA under the control of the constitutive Arabidopsis *EF1α* promoter (p*AtEF1α-MtNIP/LATD*) was introduced into *Atchl1-5* plants, with plants transformed by *AtNRT1.1* cDNA regulated by the same promoter (p*AtEF1α-AtNRT1.1*) serving as a positive control. *Atchl1-5*/p*AtEF1α-MtNIP/LATD* was found to be sensitive to chlorate, similar to the positive control *Atchl1-5* plants transformed with p*AtEF1α-AtNRT1.1* and wild-type ecotype Columbia (Col-0). Negative control mutant *Atchl1-5* plants were resistant to chlorate, as expected (Fig. 5; Supplemental Fig. S2). Wild-type Col-0 and the *Atchl1-5* plants constitutively expressing either *AtNRT1.1* or *MtNIP/LATD* showed reductions in fresh weight and chlorophyll content after chlorate treatment compared with the resistant *Atchl1-5* plants (Table II). A second independent transformed line of *Atchl1-5* transformed with p*AtEF1α-MtNIP/LATD* was also constructed and found to be chlorate sensitive as well (Supplemental Fig. S2). Therefore, we conclude that since MtNIP/LATD transports the NO_3^- analog chlorate in planta, it is extremely likely to transport NO_3^- in planta as well.

AtNRT1.1, But Not *AgDCAT1*, Partially Rescues the *M. truncatula nip-1* Phenotype

Since *MtNIP/LATD* restored chlorate sensitivity to the Arabidopsis *chl1-5* mutant, we tested whether *AtNRT1.1* would restore the *M. truncatula nip-1* mutant to its wild-type phenotype. At the time that this experiment was performed, AtNRT1.1 was the only NRT1(PTR) member known to be a high-affinity (dual-affinity) NO_3^- transporter (Tsay et al., 2007). We used composite *M. truncatula* plant hairy roots (Boisson-Dernier et al., 2001) transformed with p*AtEF1α-AtNRT1.1* as our test system. Composite plants were grown in aeroponic chambers in the absence of NO_3^-, inoculated with *S. meliloti*/p*hemA*::*lacZ* (Boivin et al., 1990), and root architecture and nodulation were evaluated at 15 d post inoculation (dpi). The results showed that *AtNRT1.1* partially restored *Mtnip-1* root architecture, increasing primary root length, LR number, and LR length to 53%, 37%, and 67% of the wild-type values, respectively (Fig. 6). However, the nodules in *Mtnip-1* plants transformed with the p*AtEF1α-AtNRT1.1* construct had an *Mtnip-1* phenotype, with the presence of brown pigments, no

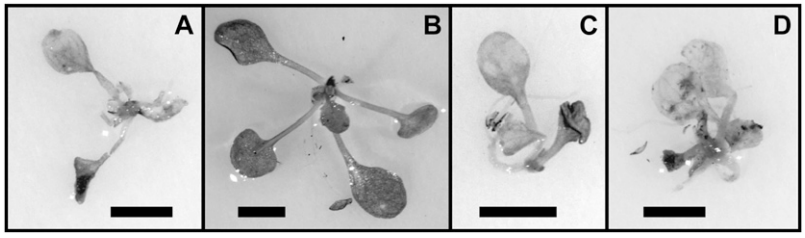

Figure 5. *MtNIP/LATD* complements the chlorate-insensitivity phenotype of the Arabidopsis *chl1-5* mutant. Arabidopsis *chl1-5* plants were transformed with a construct containing *MtNIP/LATD* cDNA under the control of the Arabidopsis *EF1α* promoter, p*AtEF1α-MtNIP/LATD*, or a positive control construct containing the Arabidopsis *AtNRT1.1* gene under the control of the same promoter, p*AtEF1α-AtNRT1.1*. The plants were treated with chlorate, a NO_3^- analog that can be converted to toxic chlorite after uptake, as described by Tsay et al. (1993). A, Arabidopsis Col-0 plant. B, Arabidopsis *chl1-5* plant. C, Arabidopsis *chl1-5*/p*AtEF1α-AtNRT1.1* plant. D, Arabidopsis *chl1-5*/p*AtEF1α-MtNIP/LATD* plant. Bars = one-quarter inch. The *MtNIP/LATD* gene was able to confer chlorate sensitivity on Arabidopsis *chl1-5* plants, similar to the *AtNRT1.1* gene.

Table II. *Fresh weight and chlorophyll content of chlorate-treated Arabidopsis plants*

Plants were grown in vermiculite:perlite (1:1) and irrigated with medium containing 5 mM NO_3^- for 5 to 7 d. Plants were then irrigated with ClO_3^--containing medium without NO_3^- for 3 d and subsequently with medium lacking both ClO_3^- and NO_3^-. Fresh weight and chlorophyll content were obtained from plants 7 to 10 d after ClO_3^- treatment. Each data point represents seven to nine plants. Two independent replicates gave similar results.

Genotype	Fresh Weight per Plant	Chlorophyll Content
	mg	*mg g^{-1} fresh wt*
Col-0	18.4 ± 1.6	1.05 ± 0.07
chl1-5	150.4 ± 6.7	2.08 ± 0.08
chl1-5/p*AtEF1α-AtNRT1.1*	20.9 ± 1.5	0.92 ± 0.06
chl1-5/p*AtEF1α-MtNIP/LATD*	21.7 ± 0.9	1.15 ± 0.15

obvious meristem, and did not differentiate into the zones that are the hallmark of N-fixing nodules (Fig. 7). Control plants transformed with p*AtEF1α-MtNIP/LATD* had wild-type phenotype nodules (Fig. 7F) and showed comparable rescue of nodulation and root architecture phenotypes as those transformed with p*MtNIP/LATD-MtNIP/LATD* (Supplemental Fig. S3), showing that use of the Arabidopsis *EF1α* promoter is not a limiting factor for complementation of the *Mtnip-1* phenotype. Overall, the experiment shows that although *AtNRT1.1* partially restores the root architecture phenotype, it is not able to restore normal nodulation to the *Mtnip-1* plants.

We also tested whether the gene encoding the alder symbiotic AgDCAT1 dicarboxylate transporter could restore normal root development or nodulation to *Mtnip-1* plants, using a similar approach as for *AtNRT1.1*, in composite transformed plants. *Mtnip-1* plants expressing *AgDCAT1* had a phenotype indistinguishable from *Mtnip-1* plants transformed with an empty vector; in contrast, *Mtnip-1* plants expressing *MtNIP/LATD* were restored to the wild type. Wild-type A17 plant phenotypes were unaffected by *AgDCAT1* expression (Supplemental Fig. S3).

DISCUSSION

The major finding of the work reported here is that MtNIP/LATD protein is a NO_3^- transporter, and its NO_3^- transport activity partially correlates with root architecture development. Our results also suggest that MtNIP/LATD has another unknown activity that is important to MtNIP/LATD's biological roles in nodule development and in the modulation of root architecture.

Data for MtNIP/LATD NO_3^- transport come from two complementary experimental approaches. When *MtNIP/LATD* is expressed in the heterologous *X. laevis* oocyte system, it enables the oocytes to transport NO_3^- in a pH-dependent manner, demonstrating that NO_3^- transport is H^+ driven (Fig. 3), similar to other NO_3^- transporters in the NRT1(PTR) family (Tsay et al., 1993). NO_3^- uptake was characterized as having a K_m of 160 μM, making it a HATS. A second line of evidence that MtNIP/LATD is a NO_3^- transporter is that its gene's constitutive expression can complement the Arabidopsis *chl1-5* mutant, containing a deletion spanning the *AtNRT1.1* gene (Muños et al., 2004). *Atchl1-5* mutants expressing *MtNIP/LATD* are susceptible to chlorate, indicating that *MtNIP/LATD* confers on them the ability to take up the herbicide chlorate, a NO_3^- analog, from the medium (Fig. 5). Both approaches showing that MtNIP/LATD transports NO_3^- indicate that the direction of NO_3^- transport is from outside to inside cells.

One might expect *Mtnip/latd* mutants to exhibit defects in NO_3^- uptake. We measured NO_3^- uptake from medium by *Mtnip-1* and *Mtnip-3* mutants and control wild-type *M. truncatula* A17 and observed no differences between the plants in NO_3^- uptake at either 250 μM or 5 mM NO_3^-, representative of HATS and LATS, respectively (Fig. 1). This suggests that MtNIP/LATD is not a rate-limiting transporter for NO_3^- uptake

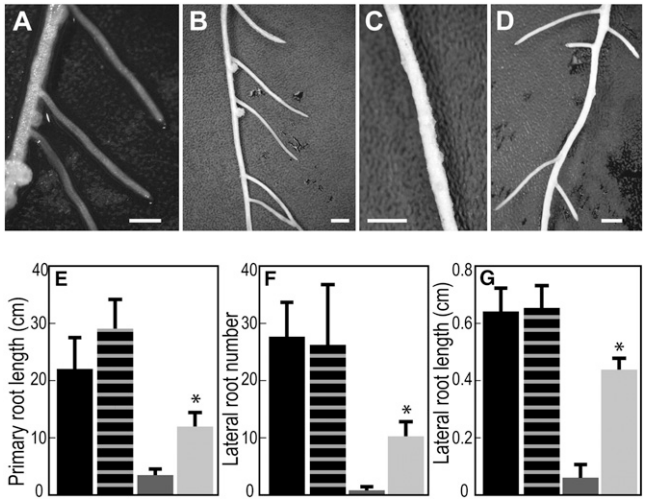

Figure 6. Arabidopsis *NRT1.1* partially complements the *M. truncatula nip-1* mutant for its root architecture phenotype. *M. truncatula nip-1* and control wild-type composite plants transformed with p*AtEF1α-AtNRT1.1* or empty pCAMBIA2301 vector, as a control, were grown in aeroponic chambers, inoculated with *S. meliloti* containing a constitutive *lacZ* gene, and grown in a 16/8-h light/dark cycle at 22°C. At 15 dpi, root architecture characteristics were evaluated. A to D, Appearance of the roots. Bars = 10 mm. A, A17, empty vector. B, A17, p*AtEF1α-AtNRT1.1*. C, *Mtnip-1*, empty vector. D, *Mtnip-1*, p*AtEF1α-AtNRT1.1*. E to G, Quantitation of primary root length (E), LR number (F), and LR length (G). Averaged values with SD are plotted ($n = 5$). Asterisks mark root attributes that are significantly different from the negative control, using Student's t test at $P < 0.01$. Black bars, A17, empty vector; vertically striped bars, A17, p*AtEF1α-AtNRT1.1*; dark gray bars, *Mtnip-1*, empty vector; light gray bars, *Mtnip-1*, p*AtEF1α-AtNRT1.1*.

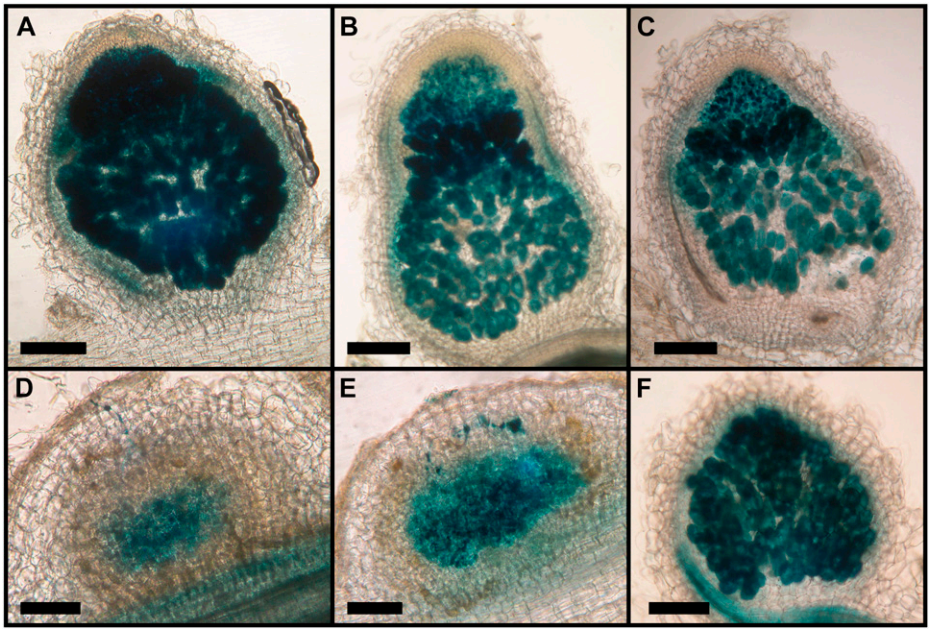

Figure 7. Arabidopsis *NRT1.1* does not complement the *M. truncatula nip-1* nodule phenotype. *M. truncatula nip-1* and control wild-type composite plants transformed with p*AtEF1α-AtNRT1.1*, empty vector pCAMBIA2301 as a negative control, or p*AtEF1α-MtNIP/LATD* were grown as in Figure 5 with *S. meliloti* containing a constitutive *lacZ* gene. At 15 dpi, nodule characteristics were evaluated after staining with X-Gal for localization of rhizobia, which stain blue. A, A17 transformed with empty vector. B, A17 transformed with p*AtEF1α-AtNRT1.1*. C, A17 transformed with p*AtEF1α-MtNIP/LATD*. D, *Mtnip-1* transformed with empty vector. E, *Mtnip-1* transformed with p*AtEF1α-AtNRT1.1*. F, *Mtnip-1* transformed with p*AtEF1α-MtNIP/LATD*. Bars = 200 μm.

into plant tissue. *MtNIP/LATD* is expressed in primary and LR tips (Yendrek et al., 2010); if MtNIP/LATD's primary biological role is to transport NO_3^-, it may constitute only a small portion of NO_3^- transport in *M. truncatula* roots. It is also possible that in *Mtnip/latd* mutants, the plant compensates by up-regulating the activity of another transporter. Another possibility is that MtNIP/LATD's transport function may be critical for redistribution of NO_3^- within the plant. We found that *Mtnip-1* is apparently normal for NO_3^- suppression of nodulation (Table I), implying that MtNIP/LATD may not be involved in this pathway (Streeter, 1988; Fei and Vessey, 2009), and/or that there are other NO_3^- transporters that can compensate for this function.

Previously, the effects of 10 and 50 mM KNO_3 on primary root length and LR density in *Mtlatd* mutants were monitored; *Mtlatd* plants, like the wild type, do not show altered LR density in response to global increases in NO_3^- (Yendrek et al., 2010). Here, we examined LR lengths of *Mtnip-1* and *Mtnip-3* plants grown in 0 μM, 250 μM, or 5 mM KNO_3 and found that the LR length phenotype was rescued for *Mtnip-3* and partially rescued for *Mtnip-1* at the 5 mM KNO_3 level but not at 250 μM KNO_3 (Fig. 2), suggesting that MtNIP/LATD might have a more biologically important role at lower NO_3^- concentrations than at higher ones. However, these experiments did not control for the effects of salt concentration on root architecture, which could have affected abscisic acid levels, leading to changes in LR lengths (Liang and Harris, 2005; Liang et al., 2007), and thus are only suggestive.

Even though NO_3^- uptake was not limited in *Mtnip/latd* mutants compared with wild-type plants, NO_3^- uptake differed when these alleles were expressed in oocytes and assayed for nitrate transport. Nitrate uptake experiments in the oocyte system showed that the protein encoded by the weakest allele, *Mtnip-3*, transported NO_3^- indistinguishably from the wild type, while the proteins encoded by the two more severe alleles, *Mtnip-1* and *Mtlatd*, did not (Fig. 4). The *Mtnip-3* mutant has a phenotype: it forms Fix+/− nodules that accumulate polyphenolics and has minor defects in root architecture, in primary root length (Teillet et al., 2008; Yendrek et al., 2010) and LR length (Fig. 2). Thus, there is a correlation between MtNIP/LATD's ability to transport NO_3^- and *Mtnip/latd* mutants' abilities to form and maintain nodule and root meristems and to form nodules invaded intracellularly by rhizobia. Despite that NO_3^- transport by Mtnip-3 protein is indistinguishable from the transport by wild-type MtNIP/LATD, *Mtnip-3* has a root and nodule phenotype. This indicates that MtNIP/LATD may have another function besides NO_3^- transport.

To further address the possible link between MtNIP/LATD and NO_3^- transport, we expressed *AtNRT1.1* in *Mtnip-1* roots. We observed that the *AtNRT1.1*-transformed *Mtnip-1* plants are partially restored for their root architecture phenotype but not for the nodulation phenotype. The use of p*AtEF1α* is not a limiting factor for phenotype rescue, since *MtNIP/LATD*, expressed under the control of the same promoter, was able to restore both the root architecture phenotype (data not shown) and the nodulation phenotype (Fig. 7). No effect was observed when *AtNRT1.1* was expressed in wild-type A17 plants (Figs. 6 and 7). This suggests that AtNRT1.1 protein's dual-affinity NO_3^- transport activity affects *Mtnip-1* root architecture and supports the idea that MtNIP/LATD's NO_3^- transport activity has a role in modulating root developmental responses. Additionally, the lack of full complementation of the root architecture defects by *AtNRT1.1* and the noncomplementation of the nodulation phenotype by *AtNRT1.1* suggest that there is a function of *MtNIP/LATD* that is different from that of *AtNRT1.1*. Alternatively, it is

possible that posttranslational regulation of AtNRT1.1 in *M. truncatula* differs from that of MtNIP/LATD, especially in nodules, and that this is the cause of AtNRT1.1's inability to complement *Mtnip-1*'s nodulation phenotype. Because AtNRT1.1 has been demonstrated to transport auxin in the absence of NO_3^- (Krouk et al., 2010b) and NO_3^- was only provided during plant transformation in these experiments, another possible explanation for the observed effects on *Mtnip*'s roots is that the partial restoration of normal root architecture was brought about by AtNRT1.1-induced changes in auxin concentration. When normally expressed in Arabidopsis, AtNRT1.1 is thought to prevent auxin accumulation at LR tips by mediating basipetal auxin transport in LRs, thus halting LR growth (Krouk et al., 2010b); this is the opposite of what we observed in the *Mtnip-1* mutant expressing *AtNRT1.1* (Fig. 6). Because our experiments used a constitutive promoter to express *AtNRT1.1*, it is possible that the perturbation of auxin gradients within the roots caused the observed changes in root architecture. It is also curious that the nodule phenotype of *Mtnip-1* plants transformed with *AtNRT1.1* is different from that of *Mtnip-3*. If the ability of *Mtnip-3* nodules to form a meristem and allow rhizobia to invade intracellularly is related to Mtnip-3 protein's ability to transport NO_3^-, one would expect to find the same phenotype in *Mtnip-1* plants transformed with AtNRT1.1 as in *Mtnip-3*, which is not the case. This finding further supports the idea that MtNIP/LATD protein's activity is more than simply NO_3^- transport and is also not explained by the spectrum of activities inherent in AtNRT1.1.

What role could MtNIP/LATD-mediated NO_3^- transport play in nodulation, root architecture development, or their regulation? MtNIP/LATD NO_3^- transport could supply N at low NO_3^-concentrations to dividing plant and bacterial cells early in nodulation, and also to differentiated nodules, at the dividing and endoreduplicating cells present in zones I and II, where *MtNIP/LATD*'s promoter is active (Yendrek et al., 2010). The *MtNIP/LATD* promoter is also active in primary root meristems, LR meristems and surrounding tissue, and MtNIP/LATD NO_3^- transport could have a similar role there. In this case, the supply of NO_3^- to these tissues would provide the N required for basic cellular functions required by dividing cells, possibly facilitating the transition from primordium to self-sustaining meristem by these nascent LR organs.

Alternately, MtNIP/LATD could transport NO_3^- as a precursor to the potent signaling molecule nitric oxide (NO) early in nodulation and LR development. NO has been detected in *M. truncatula* nodule primordia not containing intracellular rhizobia, suggesting an active NO pathway in these cells, as well as in infection threads, where NO could come from either symbiotic partner (del Giudice et al., 2011). NO has also been detected in LR primordia in tomato (*Solanum lycopersicum*; Correa-Aragunde et al., 2004). We note, however, that nodulation occurs in environmental conditions where N is limiting; indeed, our laboratory conditions for nodulation occur in N starvation. We supply 0 μM NO_3^- during nodulation, and only the trace NO_3^-, expected to be in the micromolar range, present as contaminants in nutrient media and glassware are available. If NO_3^- is supplied to dividing nodule cells, it must come from seed NO_3^- stores, which should be close to depleted by the time nodules are forming or be remobilized from other N-rich components within the plant. Another possibility is that MtNIP/LATD NO_3^- transport could participate in a proposed NO_3^--NO respiration pathway in nodules (Horchani et al., 2011; Meilhoc et al., 2011). There are several observations that argue against this: *Mtnip-3*, with functional NO_3^- transport (Fig. 4), has abnormal nodules (Teillet et al., 2008), and *MtNIP/LATD*'s promoter is active in nodule meristems and in the invasion zone but not in the N-fixing zone (Yendrek et al., 2010), suggesting that MtNIP/LATD may be absent in the N-fixing zone.

Because MtNIP/LATD may have another function besides NO_3^- transport, it is plausible that the other function is responsible for some of the *Mtnip/latd* mutants' phenotypes. Here, we have presented data suggesting that neither His nor dicarboxylates are substrates for MtNIP/LATD transport (Supplemental Table S1; Supplemental Fig. S3). We and others have speculated that MtNIP/LATD may be a NO_3^- transceptor or sensor (Harris and Dickstein, 2010; Yendrek et al., 2010; Gojon et al., 2011). If it is a NO_3^- transceptor or sensor, we predict that it may be responsible for high-affinity NO_3^- sensing. This is because it is a high-affinity transporter and because the root architecture phenotypes are partially rescued by high, but not low, NO_3^- concentrations (Fig. 2). It is also possible that MtNIP/LATD is able to transport hormones like AtNRT1.1 (Krouk et al., 2010b) and AtNRT1.2 (Kanno et al., 2012) and that this is responsible for the other function(s) of MtNIP/LATD.

MATERIALS AND METHODS

Plant Growth Conditions

Medicago truncatula A17 (wild type) and nodulation mutants were grown in aeroponic chambers with Lullien medium (Lullien et al., 1987), starved for N for 5 d, and inoculated with *Sinorhizobium medicae* strain ABS7 (Bekki et al., 1987) or *Sinorhizobium meliloti* strain Rm2011 (Rosenberg et al., 1981) harboring pXLGD4 (Boivin et al., 1990; Penmetsa and Cook, 1997), as described previously (Veereshlingam et al., 2004; Pislariu and Dickstein, 2007). For experiments where *M. truncatula* plants were grown in the presence of N sources, the relevant N sources were added to Lullien medium from the beginning of the experiment and inoculations were done with ABS7/pXLGD4. At 15 dpi, plants were stained with 5-bromo-4-chloro-3-indolyl-β-d-galactopyranoside acid (X-Gal) to identify nodules. Arabidopsis (*Arabidopsis thaliana*) plants were grown as described (Srivastava et al., 2008) at 22°C with a 16/8-h light/dark regime.

Nitrate Uptake Studies in *M. truncatula*

A17, *Mtnip-1*, and *Mtnip-3* seedlings were surface sterilized, germinated, placed on buffered nodulation medium (Ehrhardt et al., 1992) solidified with agar, pH 5.8, supplemented with 5 mM NH_4NO_3, and grown for 7 d at 22°C

with a 16/8-h light/dark regime, with roots shielded from the light. Plants were transferred to N-free buffered nodulation medium agar and grown for 3 d to starve them for N. Plants were placed in liquid buffered nodulation medium supplemented with either 250 μM or 5 mM KNO_3. Samples from the medium were collected at the indicated times and assayed for NO_3^- using the Cayman (no. 780001) NO_3^-/NO_2^- assay kit following the manufacturer's instructions.

Construction of Oocyte Expression Vectors

RNA was extracted from *M. truncatula* A17 plants and mutant *Mtnip-1*, *Mtlatd*, and *Mtnip-3* using the RNeasy kit (Qiagen). First-strand cDNA was transcribed using oligo(dT) and SuperScript III reverse transcriptase (Invitrogen), and the wild-type *MtNIP/LATD* and mutant *Mtnip/latd* cDNAs were made using *MtNIP/LATD*-specific primers NIPcEXP1R, NIPcExp1F, and NIPcDNANheI_F (Supplemental Table S2) via PCR with Phusion high-fidelity DNA polymerase (New England Biolabs). The resulting 1,776-bp cDNAs were cloned into vectors pSP64T (Krieg and Melton, 1984) and pcDNA3.1(−) (Invitrogen). *AtNRT1.1* cDNA was amplified from pMS008 (see below) using primers Chl_1F and Chl_1R, cloned into PCR8/GW/TOPO, and then moved into pOO2/GW (a gift from Dr. John Ward) downstream of an SP6 promoter. All clones were verified by DNA sequencing.

Binary Vectors

MtNIP/LATD cDNA was amplified with NIPC2F and NIPCODBst1R, digested with *Nco*I and *Bst*EII, and ligated into a vector containing the *AtEF1α* promoter engineered to contain a 5′ *Bam*HI site and a 3′ *Nco*I site, creating pMS004. Subsequently, the *AtEF1α -MtNIP/LATD* cDNA fragment was cloned into the *Bam*HI and *Bst*EII sites of binary vector pCAMBIA2301. *AtNRT1.1* cDNA was amplified from total cDNA made from wild-type Col-0 Arabidopsis mRNA using primers CHL11F and CHL11R, digested with *Bsp*HI and *Bst*EII, and cloned into *Nco*I- and *Bst*EII-digested pMS004 to obtain pMS008. The p*AtEF1α-AtNRT1.1* fragment was then subcloned into the *Bam*HI and *Bst*EII sites of pCAMBIA2301. For the p*MtNIP/LATD-MtNIP/LATD* construct, the p*AtEF1α* in pMS004 was replaced by a 3-kb upstream region of *MtNIP/LATD* amplified using NIP 10F and NIP P1R primers, followed by *Eco*RI and *Nco*I/*Bsp*HI digestion to create the pMS006 clone. Then, the pMS006 *Eco*RI/*Bst*EII fragment was moved into the *Eco*RI/*Bst*EII site of pCAMBIA2301. *AgDCAT1* cDNA was PCR amplified from pJET1.2-*AgDCAT1* (a gift of Dr. K. Pawlowski) using DC-*Bgl*II and DC-*Nhe*I primers and cloned into the *Bam*HI and *Nhe*I sites of pMS014 vector, to create pMS015. Then, the pMS015 *Eco*RI/*Bst*EII fragment was moved into the *Eco*RI/*Bst*EII site of pCAMBIA2301 to create the p*MtNIP/LATD-AgDCAT1* construct. Supplemental Table S2 contains the primer sequences.

Nitrate and His Uptake in *Xenopus laevis* Oocytes

Capped mRNA was transcribed in vitro from linearized plasmid using SP6 or T7 RNA polymerase (mMESSAGE mMACHINE; Ambion). Collagenase-treated oocytes were isolated and microinjected with approximately 50 ng of RNA in 50 nL of sterile water. Oocytes microinjected with 50 nL of sterile water were used as negative controls. Oocytes were incubated in ND96 solution (Liu and Tsay, 2003) for 24 to 40 h at 18°C. For NO_3^- uptake, oocytes were incubated in a solution containing 230 mM mannitol, 15 mM $CaCl_2$, and 10 mM HEPES (pH 7.4), containing various KNO_3 concentrations at pH 5.5 or 7.4, at 16°C for the indicated times. After incubation, batches of four to six oocytes were lysed in 40 μL of water, centrifuged at 13,500*g* for 20 min, and the supernatant was analyzed for NO_3^- content as above. For His uptake, oocytes were incubated in ND96 medium, pH 5.5, at 25°C containing 1 mM uniformly ^{13}C-labeled His (Cambridge Isotope). After incubation, oocytes were washed five times with the same medium containing 10 mM unlabeled His (Sigma-Aldrich), and batches of eight oocytes were lysed in 100 μL of water and centrifuged at 13,500*g* for 20 min. The supernatant was lyophilized to 15 μL and analyzed using ultraperformance liquid chromatography-electrospray ionization-tandem mass spectrometry (UPLC-ESI-MS/MS).

UPLC-ESI-MS/MS Analysis

[$^{13}C_6$]His was quantified using a precolumn derivatization method with 6-aminoquinolyl-*N*-hydroxysuccinimidyl carbamate (AQC) combined with UPLC-ESI-MS/MS. AQC derivatization was performed using the AccQ•Tag derivatization kit (Waters) according to the manufacturer's protocol. UPLC-ESI-MS/MS analysis was carried out on a Waters Acquity UPLC system interfaced to a Waters Xevo TQ mass spectrometer as described (Salazar et al., 2012). Briefly, the AQC-derivatized [$^{13}C_6$]His was separated on a Waters AccQ•Tag Ultra column (2.1 mm i.d. × 100 mm, 1.7-μm particles) using AccQ•Tag Ultra eluents (Waters) and a gradient described earlier (Salazar et al., 2012). The sample injection volume was 1 μL, the UPLC column flow rate was 0.7 mL min^{-1}, and the column temperature was 55°C. Mass spectra were acquired using positive ESI and the multiple reaction monitoring mode, with the following ionization source settings: capillary voltage, 1.99 kV (ESI+); desolvation temperature, 650°C; desolvation gas flow rate, 1,000 L h^{-1}; source temperature, 150°C. Argon was used as the collision gas at a flow rate of 0.15 mL min^{-1}. The collision energy and cone voltage were optimized for the derivatized [$^{13}C_6$]His using the IntelliStart software (collision energy = 26 eV; cone voltage = 20 V). The most sensitive parent-daughter ion transition of derivatized His (mass-to-charge ratio 332.1 > 171.0) was selected for quantitation. The mass spectrometer response was calibrated by injecting AQC-derivatized [$^{13}C_6$]His standard solutions of known concentration. The UPLC-ESI-MS/MS system control and data acquisition were performed with Waters MassLynx software. Data analysis was conducted with TargetLynx software (Waters).

Transformation of *Atchl1-5* Plants with the *MtNIP/LATD* Expression Construct

The *MtNIP/LATD* expression construct (p*AtEF1α-MtNIP/LATD*) was transformed into the *Agrobacterium tumefaciens* GV3101(pMP90) strain by electroporation. Positive colonies were selected by colony PCR, verified by restriction digestion, and transformed into the *Atchl1-5* mutant (Tsay et al., 1993) by the floral dip method (Clough and Bent, 1998). Seeds were collected, and transformed plants were selected on kanamycin medium. Two independent homozygous transformed lines of *Atchl1-5* transformed with p*AtEF1α-MtNIP/LATD* were selected.

Chlorate Sensitivity Test

Plants were grown in vermiculite:perlite (1:1 mixture) under continuous illumination at 25°C to 27°C. Plants were irrigated every 2 to 3 d with medium containing 10 mM KH_2PO_4 (pH 5.3), 5 mM KNO_3, 2 mM $MgSO_4$, 1 mM $CaCl_2$, 0.1 mM FeEDTA, 50 pM H_3BO_3, 12 pM $MnSO_4$, 1 pM ZnCl, 1 pM $CuSO_4$, and 0.2 pM Na_2MoO_4. At 5 to 7 d post germination, plants were irrigated twice with medium containing 2 mM $NaClO_3$ without NO_3^-. Three days after ClO_3^- treatment, plants were switched to irrigation medium lacking ClO_3^- and NO_3^-. Plants were examined 7 to 10 d after ClO_3^- treatment for necrosis and bleaching symptoms characteristic of chlorate toxicity (Wilkinson and Crawford, 1991), and their fresh weights and chlorophyll contents were obtained. Digital color photographs of the plants were obtained, corrected for color balance (Supplemental Fig. S2), converted to grayscale, and corrected for contrast (Fig. 5) using Photoshop (Adobe Software).

Chlorophyll content was determined from approximately 10 mg of fresh leaves that were weighed, frozen in liquid N_2, ground to a fine powder, added to tubes with 100 μL of water and 8 mL of 96% ethanol, and mixed. The tubes were kept at 25°C overnight, mixed again, and the particulates were allowed to settle. The absorbance was recorded at 648.6 and 664.2 nm. Total chlorophyll was calculated as described (Lichtenthaler, 1987).

M. truncatula Root Transformation

Vectors containing the expression constructs were transformed into *Agrobacterium rhizogenes* ARqua1 strain (Quandt et al., 1993) by the freeze-thaw method (Höfgen and Willmitzer, 1988). Positive ARqua1 colonies were transformed into *Mtnip-1* and A17 plants by the needle-poking method (Mortier et al., 2010).

Analysis of LRs and Nodules in Transformed Plants

Root nodules were analyzed at 12 dpi. They were stained with X-Gal for *lacZ*, present in p*XLGD4* plasmid in *S. medicae* ABS7 and mounted in 2.5% low melting point agarose; 50-μm sections were obtained using a 1000 Plus Vibratome (Vibratome) and observed by light microscopy. LRs were inspected visually and with a dissecting microscope.

The *MtNIP/LATD* sequence may be found under GenBank accession no. GQ401665.

Supplemental Data

The following materials are available in the online version of this article.

Supplemental Figure S1. Comparison of nitrate uptake in oocytes expressing *MtNIP/LATD* versus *AtNRT1.1*.

Supplemental Figure S2. *MtNIP/LATD* complements the chlorate-insensitivity phenotype of the Arabidopsis *chl1-5* mutant.

Supplemental Figure S3. *AgDCAT1* does not complement the *Mtnip-1* mutant.

Supplemental Table S1. *MtNIP/LATD*-expressing oocytes do not take up His.

Supplemental Table S2. Sequences of oligonucleotide primers used in this study.

ACKNOWLEDGMENTS

We thank Pudur Jagadeeswaran, Tina Machu, and their laboratories for help with the *X. laevis* oocyte experiments, John Ward for vector pOO2/GW and suggestions about oocytes, Jeanne Harris for helpful discussions, Brian Ayre and his laboratory for help with Arabidopsis transformation, Nigel Crawford for Arabidopsis *chl1-5* seeds, Katharina Pawlowski for the *AgDCAT1* cDNA, and Jyoti Shah and Jeremy Murray for critical reading of the manuscript.

Received February 27, 2012; accepted August 1, 2012; published August 2, 2012.

LITERATURE CITED

Almagro A, Lin SH, Tsay Y-F (2008) Characterization of the *Arabidopsis* nitrate transporter NRT1.6 reveals a role of nitrate in early embryo development. Plant Cell **20:** 3289–3299

Barbier-Brygoo H, De Angeli A, Filleur S, Frachisse J-M, Gambale F, Thomine S, Wege S (2011) Anion channels/transporters in plants: from molecular bases to regulatory networks. Annu Rev Plant Biol **62:** 25–51

Bekki A, Trinchant J-C, Rigaud J (1987) Nitrogen fixation (C_2H_2 reduction) by *Medicago* nodules and bacteroids under sodium chloride stress. Physiol Plant **71:** 61–67

Benedito VA, Li H, Dai X, Wandrey M, He J, Kaundal R, Torres-Jerez I, Gomez SK, Harrison MJ, Tang Y, et al (2010) Genomic inventory and transcriptional analysis of *Medicago truncatula* transporters. Plant Physiol **152:** 1716–1730

Boisson-Dernier A, Chabaud M, Garcia F, Bécard G, Rosenberg C, Barker DG (2001) *Agrobacterium rhizogenes*-transformed roots of *Medicago truncatula* for the study of nitrogen-fixing and endomycorrhizal symbiotic associations. Mol Plant Microbe Interact **14:** 695–700

Boivin C, Camut S, Malpica CA, Truchet G, Rosenberg C (1990) *Rhizobium meliloti* genes encoding catabolism of trigonelline are induced under symbiotic conditions. Plant Cell **2:** 1157–1170

Bright L, Liang Y, Mitchell DM, Harris JM (2005) The *LATD* gene of *Medicago truncatula* is required for both nodule and root development. Mol Plant Microbe Interact **18:** 521–532

Clough SJ, Bent AF (1998) Floral dip: a simplified method for *Agrobacterium*-mediated transformation of *Arabidopsis thaliana*. Plant J **16:** 735–743

Correa-Aragunde N, Graziano M, Lamattina L (2004) Nitric oxide plays a central role in determining lateral root development in tomato. Planta **218:** 900–905

Crawford NM (1995) Nitrate: nutrient and signal for plant growth. Plant Cell **7:** 859–868

Criscuolo G, Valkov VT, Parlati A, Alves LM, Chiurazzi M (2012) Molecular characterization of the *Lotus japonicus NRT1(PTR)* and *NRT2* families. Plant Cell Environ **35:** 1567–1581

del Giudice J, Cam Y, Damiani I, Fung-Chat F, Meilhoc E, Bruand C, Brouquisse R, Puppo A, Boscari A (2011) Nitric oxide is required for an optimal establishment of the *Medicago truncatula-Sinorhizobium meliloti* symbiosis. New Phytol **191:** 405–417

Doddema H, Hofstra JJ, Feenstra WJ (1978) Uptake of nitrate by mutants of *Arabidopsis thaliana*, disturbed in uptake or reduction of nitrate. Physiol Plant **43:** 343–350

Ehrhardt DW, Atkinson EM, Long SR (1992) Depolarization of alfalfa root hair membrane potential by *Rhizobium meliloti* Nod factors. Science **256:** 998–1000

Fan S-C, Lin C-S, Hsu PK, Lin S-H, Tsay Y-F (2009) The *Arabidopsis* nitrate transporter NRT1.7, expressed in phloem, is responsible for source-to-sink remobilization of nitrate. Plant Cell **21:** 2750–2761

Fei H, Vessey JK (2009) Stimulation of nodulation in *Medicago truncatula* by low concentrations of ammonium: quantitative reverse transcription PCR analysis of selected genes. Physiol Plant **135:** 317–330

Gojon A, Krouk G, Perrine-Walker F, Laugier E (2011) Nitrate transceptor (s) in plants. J Exp Bot **62:** 2299–2308

Harris JM, Dickstein R (2010) Control of root architecture and nodulation by the *LATD/NIP* transporter. Plant Signal Behav **5:** 1365–1369

Ho C-H, Lin S-H, Hu H-C, Tsay Y-F (2009) CHL1 functions as a nitrate sensor in plants. Cell **138:** 1184–1194

Höfgen R, Willmitzer L (1988) Storage of competent cells for *Agrobacterium* transformation. Nucleic Acids Res **16:** 9877

Horchani F, Prévot M, Boscari A, Evangelisti E, Meilhoc E, Bruand C, Raymond P, Boncompagni E, Aschi-Smiti S, Puppo A, et al (2011) Both plant and bacterial nitrate reductases contribute to nitric oxide production in *Medicago truncatula* nitrogen-fixing nodules. Plant Physiol **155:** 1023–1036

Huang N-C, Chiang C-S, Crawford NM, Tsay Y-F (1996) *CHL1* encodes a component of the low-affinity nitrate uptake system in *Arabidopsis* and shows cell type-specific expression in roots. Plant Cell **8:** 2183–2191

Jeong J, Suh S, Guan C, Tsay Y-F, Moran N, Oh CJ, An C-S, Demchenko KN, Pawlowski K, Lee Y (2004) A nodule-specific dicarboxylate transporter from alder is a member of the peptide transporter family. Plant Physiol **134:** 969–978

Kanno Y, Hanada A, Chiba Y, Ichikawa T, Nakazawa M, Matsui M, Koshiba T, Kamiya Y, Seo M (2012) Identification of an abscisic acid transporter by functional screening using the receptor complex as a sensor. Proc Natl Acad Sci USA **109:** 9653–9658

Kouchi H, Imaizumi-Anraku H, Hayashi M, Hakoyama T, Nakagawa T, Umehara Y, Suganuma N, Kawaguchi M (2010) How many peas in a pod? Legume genes responsible for mutualistic symbioses underground. Plant Cell Physiol **51:** 1381–1397

Krieg PA, Melton DA (1984) Functional messenger RNAs are produced by SP6 *in vitro* transcription of cloned cDNAs. Nucleic Acids Res **12:** 7057–7070

Krouk G, Crawford NM, Coruzzi GM, Tsay YF (2010a) Nitrate signaling: adaptation to fluctuating environments. Curr Opin Plant Biol **13:** 266–273

Krouk G, Lacombe B, Bielach A, Perrine-Walker F, Malinska K, Mounier E, Hoyerova K, Tillard P, Leon S, Ljung K, et al (2010b) Nitrate-regulated auxin transport by NRT1.1 defines a mechanism for nutrient sensing in plants. Dev Cell **18:** 927–937

Li J-Y, Fu Y-L, Pike SM, Bao J, Tian W, Zhang Y, Chen C-Z, Zhang Y, Li H-M, Huang J, et al (2010) The *Arabidopsis* nitrate transporter NRT1.8 functions in nitrate removal from the xylem sap and mediates cadmium tolerance. Plant Cell **22:** 1633–1646

Liang Y, Harris JM (2005) Response of root branching to abscisic acid is correlated with nodule formation both in legumes and nonlegumes. Am J Bot **92:** 1675–1683

Liang Y, Mitchell DM, Harris JM (2007) Abscisic acid rescues the root meristem defects of the *Medicago truncatula latd* mutant. Dev Biol **304:** 297–307

Lichtenthaler HK (1987) Chlorophylls and carotenoids: pigments of photosynthetic biomembranes. Methods Enzymol **148:** 350–382

Lin S-H, Kuo H-F, Canivenc G, Lin C-S, Lepetit M, Hsu P-K, Tillard P, Lin H-L, Wang Y-Y, Tsai CB, et al (2008) Mutation of the *Arabidopsis NRT1.5* nitrate transporter causes defective root-to-shoot nitrate transport. Plant Cell **20:** 2514–2528

Linkohr BI, Williamson LC, Fitter AH, Leyser HMO (2002) Nitrate and phosphate availability and distribution have different effects on root system architecture of *Arabidopsis*. Plant J **29:** 751–760

Liu K-H, Tsay Y-F (2003) Switching between the two action modes of the dual-affinity nitrate transporter CHL1 by phosphorylation. EMBO J **22:** 1005–1013

Lullien V, Barker DG, de Lajudie P, Huguet T (1987) Plant gene expression in effective and ineffective root nodules of alfalfa (*Medicago sativa*). Plant Mol Biol **9:** 469–478

Meilhoc E, Boscari A, Bruand C, Puppo A, Brouquisse R (2011) Nitric oxide in legume-rhizobium symbiosis. Plant Sci **181:** 573–581

Miller AJ, Fan X, Orsel M, Smith SJ, Wells DM (2007) Nitrate transport and signalling. J Exp Bot **58:** 2297–2306

Miranda M, Borisjuk L, Tewes A, Dietrich D, Rentsch D, Weber H, Wobus U (2003) Peptide and amino acid transporters are differentially regulated during seed development and germination in faba bean. Plant Physiol **132:** 1950–1960

Morère-Le Paven M-C, Viau L, Hamon A, Vandecasteele C, Pellizzaro A, Bourdin C, Laffont C, Lapied B, Lepetit M, Frugier F, et al (2011) Characterization of a dual-affinity nitrate transporter MtNRT1.3 in the model legume *Medicago truncatula*. J Exp Bot **62:** 5595–5605

Mortier V, Den Herder G, Whitford R, Van de Velde W, Rombauts S, D'Haeseleer K, Holsters M, Goormachtig S (2010) CLE peptides control *Medicago truncatula* nodulation locally and systemically. Plant Physiol **153:** 222–237

Muños S, Cazettes C, Fizames C, Gaymard F, Tillard P, Lepetit M, Lejay L, Gojon A (2004) Transcript profiling in the *chl1-5* mutant of *Arabidopsis* reveals a role of the nitrate transporter NRT1.1 in the regulation of another nitrate transporter, NRT2.1. Plant Cell **16:** 2433–2447

Oldroyd GED, Downie JA (2008) Coordinating nodule morphogenesis with rhizobial infection in legumes. Annu Rev Plant Biol **59:** 519–546

Penmetsa RV, Cook DR (1997) A legume ethylene-insensitive mutant hyperinfected by its rhizobial symbiont. Science **275:** 527–530

Pislariu CI, Dickstein R (2007) An *IRE*-like AGC kinase gene, *MtIRE*, has unique expression in the invasion zone of developing root nodules in *Medicago truncatula*. Plant Physiol **144:** 682–694

Quandt HJ, Puhler A, Broer I (1993) Transgenic root nodules of *Vicia hirsuta*: a fast and efficient system for the study of gene expression in indeterminate-type nodules. Mol Plant Microbe Interact **6:** 699–706

Remans T, Nacry P, Pervent M, Filleur S, Diatloff E, Mounier E, Tillard P, Forde BG, Gojon A (2006) The *Arabidopsis* NRT1.1 transporter participates in the signaling pathway triggering root colonization of nitrate-rich patches. Proc Natl Acad Sci USA **103:** 19206–19211

Rosenberg C, Boistard P, Dénarié J, Casse-Delbart F (1981) Genes controlling early and late functions in symbiosis are located on a megaplasmid in *Rhizobium meliloti*. Mol Gen Genet **184:** 326–333

Salazar C, Armenta JM, Cortés DF, Shulaev V (2012) Combination of an AccQ·Tag-ultra performance liquid chromatographic method with tandem mass spectrometry for the analysis of amino acids. Methods Mol Biol **828:** 13–28

Sato S, Nakamura Y, Kaneko T, Asamizu E, Kato T, Nakao M, Sasamoto S, Watanabe A, Ono A, Kawashima K, et al (2008) Genome structure of the legume, *Lotus japonicus*. DNA Res **15:** 227–239

Schmutz J, Cannon SB, Schlueter J, Ma J, Mitros T, Nelson W, Hyten DL, Song Q, Thelen JJ, Cheng J, et al (2010) Genome sequence of the palaeopolyploid soybean. Nature **463:** 178–183

Segonzac C, Boyer J-C, Ipotesi E, Szponarski W, Tillard P, Touraine B, Sommerer N, Rossignol M, Gibrat R (2007) Nitrate efflux at the root plasma membrane: identification of an *Arabidopsis* excretion transporter. Plant Cell **19:** 3760–3777

Srivastava AC, Ganesan S, Ismail IO, Ayre BG (2008) Functional characterization of the Arabidopsis AtSUC2 sucrose/H^+ symporter by tissue-specific complementation reveals an essential role in phloem loading but not in long-distance transport. Plant Physiol **148:** 200–211

Streeter J (1988) Inhibition of legume nodule formation and N_2 fixation by nitrate. CRC Crit Rev Plant Sci **7:** 1–23

Teillet A, Garcia J, de Billy F, Gherardi M, Huguet T, Barker DG, de Carvalho-Niebel F, Journet E-P (2008) *api*, a novel *Medicago truncatula* symbiotic mutant impaired in nodule primordium invasion. Mol Plant Microbe Interact **21:** 535–546

Tsay Y-F, Chiu C-C, Tsai C-B, Ho C-H, Hsu P-K (2007) Nitrate transporters and peptide transporters. FEBS Lett **581:** 2290–2300

Tsay Y-F, Schroeder JI, Feldmann KA, Crawford NM (1993) The herbicide sensitivity gene *CHL1* of Arabidopsis encodes a nitrate-inducible nitrate transporter. Cell **72:** 705–713

Udvardi MK, Day DA (1997) Metabolite transport across symbiotic membranes of legume nodules. Annu Rev Plant Physiol Plant Mol Biol **48:** 493–523

Veereshlingam H, Haynes JG, Penmetsa RV, Cook DR, Sherrier DJ, Dickstein R (2004) *nip*, a symbiotic *Medicago truncatula* mutant that forms root nodules with aberrant infection threads and plant defense-like response. Plant Physiol **136:** 3692–3702

Walch-Liu P, Forde BG (2008) Nitrate signalling mediated by the NRT1.1 nitrate transporter antagonises L-glutamate-induced changes in root architecture. Plant J **54:** 820–828

Walch-Liu P, Liu L-H, Remans T, Tester M, Forde BG (2006) Evidence that L-glutamate can act as an exogenous signal to modulate root growth and branching in *Arabidopsis thaliana*. Plant Cell Physiol **47:** 1045–1057

Wang R, Xing X, Wang Y, Tran A, Crawford NM (2009) A genetic screen for nitrate regulatory mutants captures the nitrate transporter gene *NRT1.1*. Plant Physiol **151:** 472–478

Wang Y-Y, Tsay Y-F (2011) *Arabidopsis* nitrate transporter NRT1.9 is important in phloem nitrate transport. Plant Cell **23:** 1945–1957

Waterworth WM, Bray CM (2006) Enigma variations for peptides and their transporters in higher plants. Ann Bot (Lond) **98:** 1–8

White J, Prell J, James EK, Poole P (2007) Nutrient sharing between symbionts. Plant Physiol **144:** 604–614

Wilkinson JQ, Crawford NM (1991) Identification of the *Arabidopsis CHL3* gene as the nitrate reductase structural gene *NIA2*. Plant Cell **3:** 461–471

Xu G, Fan X, Miller AJ (2012) Plant nitrogen assimilation and use efficiency. Annu Rev Plant Biol **63:** 5.1–5.30

Yamashita T, Shimada S, Guo W, Sato K, Kohmura E, Hayakawa T, Takagi T, Tohyama M (1997) Cloning and functional expression of a brain peptide/histidine transporter. J Biol Chem **272:** 10205–10211

Yendrek CR, Lee Y-C, Morris V, Liang Y, Pislariu CI, Burkart G, Meckfessel MH, Salehin M, Kessler H, Wessler H, et al (2010) A putative transporter is essential for integrating nutrient and hormone signaling with lateral root growth and nodule development in *Medicago truncatula*. Plant J **62:** 100–112

Yokoyama T, Kodama N, Aoshima H, Izu H, Matsushita K, Yamada M (2001) Cloning of a cDNA for a constitutive NRT1 transporter from soybean and comparison of gene expression of soybean NRT1 transporters. Biochim Biophys Acta **1518:** 79–86

Young ND, Debellé F, Oldroyd GED, Geurts R, Cannon SB, Udvardi MK, Benedito VA, Mayer KFX, Gouzy J, Schoof H, et al (2011) The *Medicago* genome provides insight into the evolution of rhizobial symbioses. Nature **480:** 520–524

Zhang H, Forde BG (2000) Regulation of *Arabidopsis* root development by nitrate availability. J Exp Bot **51:** 51–59

Zhao X, Huang J, Yu H, Wang L, Xie W (2010) Genomic survey, characterization and expression profile analysis of the peptide transporter family in rice (*Oryza sativa* L.). BMC Plant Biol **10:** 92

Zhou J-J, Theodoulou FL, Muldin I, Ingemarsson B, Miller AJ (1998) Cloning and functional characterization of a *Brassica napus* transporter that is able to transport nitrate and histidine. J Biol Chem **273:** 12017–12023

Zifarelli G, Pusch M (2010) CLC transport proteins in plants. FEBS Lett **584:** 2122–2127